Impact of ontogenic changes on the dynamics of a fungal crop disease model motivated by coffee leaf rust

Clotilde Djuikem, Frédéric Grognard, Suzanne Touzeau

Impact of ontogenic changes on the dynamics of a fungal crop disease model motivated by coffee leaf rust

Clotilde Djuikem[1*], Frédéric Grognard[1] and Suzanne Touzeau[1,2]

[1] Université Côte d'Azur, Inria, INRAE, CNRS, MACBES, France.
[2]Université Côte d'Azur, INRAE, ISA, France.

*Corresponding author(s). E-mail(s): clotilde.djuikem@inria.fr;
Contributing authors: frederic.grognard@inria.fr;
suzanne.touzeau@inria.fr;

Abstract

Ontogenic resistance has been described for many plant-pathogen systems. Conversely, coffee leaf rust, a major fungal disease that drastically reduces coffee production, exhibits a form of ontogenic susceptibility, with a higher infection risk for mature leaves. To take into account stage-dependent crop response to phytopathogenic fungi, we developed an SEIR-U epidemiological model, where U stands for spores, which differentiates between young and mature leaves. Based on this model, we also explored the impact of ontogenic resistance on the sporulation rate. We computed the basic reproduction number $\boldsymbol{\mathcal{R}_0}$, which classically determines the stability of the disease-free equilibrium. We identified forward and backward bifurcation cases. The backward bifurcation is generated by the high sporulation of young leaves compared to mature ones. In this case, when the basic reproduction number is less than one, the disease can persist. These results provide useful insights on the disease dynamics and its control. In particular, ontogenic resistance may require higher control efforts to eradicate the disease.

Keywords: Epidemiological model Host age classes Coffee leaf rust Ontogenic resistance Basic reproduction number Backward bifurcation

MSC Classification: 92D30 37N25 34D20 34C23 34C60

Paper published in *Journal of Mathematical Biology* (2024) 88:30
DOI: 10.1007/s00285-024-02053-4

1 Introduction

Plant pest and pathogens account for up to 40% of yield loss worldwide (Boonekamp, 2012). In the current context of ever growing population and climate change, they are major issues to ensure food security. Hence, the interactions between pest/pathogens and their hosts need to be better understood. Mathematical models of fungal diseases have received a lot of attention from researchers. For instance, Fleming (1980) used a mathematical model to describe the transition of a cereal rust population from endemic to epidemic densities and prove that natural enemies are likely to control only low-density cereal rust populations. Pivonia and Yang (2006) studied the seasonal appearance of rusts in the United States, in particular soybean rust, thanks to a general disease model. Rimbaud et al (2018) investigated how the spatial deployment of resistant cultivars affected the resistance efficiency and durability, using a demogenetic model, for a seasonal crop infected by a fungal-like pathogen.

There are fewer models of fungal diseases that target perennial hosts. For instance, Burie et al (2008) explored the dynamical behaviour of mildew in a vineyard, while Mammeri et al (2014a) studied the impact of spatial heterogeneities on its spread and control during a cropping season. Djidjou-Demasse et al (2022) analyzed a non-local spatial epidemic model presenting the diffusion process of a spore producing plant pathogen responsible of one of the most destructive cocoa pods disease. Sapoukhina et al (2010) studied susceptible and resistant crop mixtures for a fungal disease propagated by airborne spores in a field. Desprez-Loustau et al (2019) developed a seasonal eco-evolutionary model of oak powdery mildew in Europe, based on a within-season and between-season transmission trade-off, which captures the main features of the disease, that is seasonality and pathogen species coexistence. Ravigné et al (2017) looked at the impact of sexual and asexual reproduction on the epidemiological dynamics of fungal plant parasites and showed that they could induce cyclic persistence of the disease, which can occur with Sigatoka diseases of banana.

In this paper, we develop an epidemiological model to describe the spread of a fungal disease on a perennial plant in an agriculture context. The originality of this model is that it is structured to represent host developmental stages, as they often impact the aggressiveness of the pathogen, stemming from nutrient availability (Coleman, 1986) or presence of different defense compounds (Maupetit et al, 2018) in the host. A susceptible host can develop resistance to a pathogen at a certain developmental stage in several plant-pathogen interactions (Develey-Rivière and Galiana, 2007). It is possible to define this age-related resistance, also known as ontogenic resistance (when old tissues are resistant), as the dynamic modification of tissue susceptibility during organ development that results in resistance to pathogenic microorganisms (Calonnec et al, 2018). Ontogenic resistance has been described for many plant-pathogen systems, namely grapevine-powder mildew (Mammeri et al, 2014b; Burie et al, 2011), strawberry-powdery mildew (Carisse and Bouchard,

2010), cocoa—Phytophthora megakarya (Soh et al, 2013). Ontogenic susceptibility occurs when old tissues are more susceptible than young ones. There are presently very few studies of this phenomenon, mostly linked to fruit maturation, such as in Ripe Rot-grapevine clusters (Cosseboom and Hu, 2022).

The present work is motivated by the particular case of coffee leaf rust (CLR) on the coffee tree, which is a perennial plant that can be exploited commercially during about 30 years (Wintgens, 2009). CLR has a major impact on coffee production (Zambolim, 2016). However, our study can be applied to other fungal diseases that target perennial hosts since most fungal diseases present the same type of life cycle, going through spore dispersion for asexual and/or sexual reproduction. CLR is caused by a basidiomycete fungus, *Hemileia vastatrix*, which infects coffee leaves of all stages, and dries them up before they fall down. The life cycle of *H. vastatrix* starts with the dispersion of uredospores, which land on the leaves. They germinate and penetrate the leaf, the infection process requires 48 hours to 10 days (Nutman et al, 1963) depending of the age of the leaf and the climatic conditions (Razafindramamba, 1958). Two to three weeks after the infection, yellow spots appear on the leaves. They grow and sporulate for two weeks to several months to produce two types of spores: uredospores for asexual reproduction and teliospores for sexual reproduction (Waller, 1982). As the teliospore part of the cycle is not well known, except that these spores do not infect coffee leaves and might even be a dead end (Koutouleas et al, 2019), it is not included in our model. For other rusts such as poplar rust, this part of the cycle is crucial for overwintering (Hacquard et al, 2011).

Mathematical models have been developed to study the epidemiology of CLR. Avelino et al (2006) investigated the factors (coffee tree characteristics, crop management patterns, environment) that affect CLR intensity in several plots in Honduras. They showed that coffee rust development is linked to three sets of factors: the environment, plant growth and development, and grower practices. Bebber et al (2016) determined the germination and infection risk depending on the climate in Colombia and neighbouring countries, based upon existing experimental data. Vandermeer et al (2018) represented the CLR dynamics in a coffee farm in Chiapas using an SI epidemiological model of the host. They showed that the network approach can be a useful way of gaining qualitative insight on spatial disease dynamics. They also showed in their study that coffee rust pattern suggests something other than random dispersal of spores. Djuikem et al (2021) studied the dynamics of CLR in a coffee plantation. However, existing models do not explicitly incorporate coffee plant development. In particular, in these models the differences between young and mature leaves are not considered while they clearly have an impact on the severity of infection. It was experimentally shown by Avelino et al (2006) and Eskes (1983) that leaves exhibit ontogenic susceptibility to CLR: with leaves developing berries (mature leaves) are more susceptible to CLR than those of the same plants without berries (young leaves). This was determined by an increased infection frequency and a decreased latency period. In this

study we considered that mature leaves became infected more quickly than young ones and supposed that young and mature leaves have the same latency period. We also assumed that the sporulation period was the same for young and mature leaves, but explored both cases for the sporulation rate, either higher or lower for mature leaves, which corresponds to ontogenic susceptibility or resistance, respectively.

Our aim is to understand the host-pathogen interactions and study the impact of ontogenic susceptibility or resistance of the host. To do so, we developed a crop-fungus interaction model using ordinary differential equations. As in classical epidemiological models, the host population was subdivided by health status, considering the crop leaf as an individual. The infection being mediated by fungus spores released in the plantation, their dynamics were also included. Moreover, this model differentiated between young and mature leaves, to take into account variations in fungus aggressiveness according to host development, in particular on the infection and sporulation rates. The model is based on the SEIR-U epidemiological model, where U stands for uredospores, presented in Djuikem et al (2021). Compared to this previous work, this new model does not include the spatially-explicit spore dispersal, but it differentiates young and mature leaves and the young leaves grow logistically. We explicitly include a berry compartment to study the impact of CLR on crop production. Secondly, we analyse the equilibria of this complex ODE model and their stability. The model takes into account the non-constant recruitment of young susceptible leaves, which are generated by mature leaves. Due to competition, the dynamics of young leaves are negatively impacted by mature leaves.

Although the germination rate (which determines the infection success) differs between young and mature leaves and is higher for mature leaves, both face the same force of infection. The latter is proportional to the number of uredospores and inversely proportional to the total number of leaves. Thus, the force of infection is frequency-dependent (Arino and McCluskey, 2010).

This paper is organized as follows. Section 2 is devoted to the formulation of the model and derive its basic properties. In Section 3, we compute the disease free equilibrium and the basic reproduction number which determines its stability. In Section 4, we prove the existence of endemic equilibria and study their stability. We also present different types of bifurcations that occur in the model. Finally, we conclude the paper and propose several perspectives for future work.

2 Model formulation and basic properties

2.1 Formulation of CLR-model

Herein, we formulate a mathematical model for the CLR in the coffee plantation. To do so, we propose an ODE coffee–CLR interaction model that takes into account the non-constant recruitment of young susceptible leaves, which are generated by mature leaves. Due to competition, the dynamics of young

leaves are negatively impacted by mature leaves and the uredospores are produce by all types of infectious leaves. More precisely, we consider that in a coffee plantation we can find: susceptible young and mature leaves (J_S and M_S), that have not (yet) been attacked, latent young and mature leaves (J_L and M_L), that are infected but not (yet) infectious, infectious young and mature leaves (J_I and M_I), dry leaves (M_R), uredospores (U), which the fungus *H. vastatrix* uses for its asexual reproduction, and berries (B).

Figure 1 gives the compartmental representation of the corresponding ODE model.

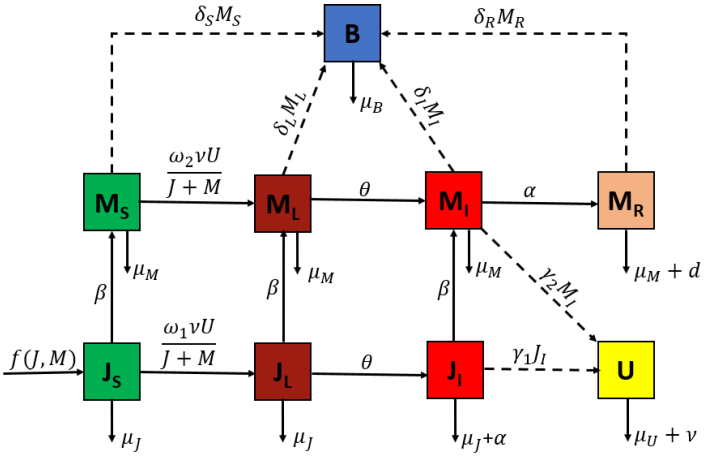

Fig. 1 Diagram of the CLR propagation in the coffee plantation corresponding to system (1). State variables are: susceptible young and mature leaves (J_S and M_S), latent young and mature leaves (J_L and M_L), infectious young and mature leaves (J_I and M_I), dry leaves (M_R), uredospores (U) and berries (B).

The process begins with a logistic-like production of susceptible young leaves at rate $r_0 M_1 - r_1 M J_S$. In the first term, $M_1 = M_S + M_L + \varepsilon(M_I + M_R)$ and $\varepsilon < 1$, since all mature leaves can produce young ones, with the infectious and dry leaves producing less due to infection. The second term represents the competition between susceptible young leaves and all mature leaves with $M = M_S + M_L + M_I + M_R$. All young leaves become mature at rate β. Uredospores land on leaves at deposition rate ν. As we assumed that the coffee plantation is dense, we chose frequency-dependent infection functions (Ravigné et al, 2017) of fractions $\frac{J_S}{J+M}$ and $\frac{M_S}{J+M}$ on young and mature leaves, respectively, with $J = J_S + J_L + J_I$. Uredospores germinate at rates ω_1 and ω_2, respectively, with $\omega_2 > \omega_1$ due to the higher infection risk of mature leaves. Young and mature latent leaves become infectious at rate θ, where $1/\theta$ corresponds to the average latency period. Infectious leaves sporulate over on average period $1/\alpha$; young leaves then die at the end of the sporulation period and hence will not produce berries, while mature ones become dry but can still produce berries in the M_R state. This explains the asymmetry between the

young and mature stages in the model. All young and mature leaves undergo natural mortality with baseline rate μ_J and μ_M, respectively. Dry leaves have an additional mortality rate d. Uredospores are produced by infectious young and mature leaves at rate γ_1 and γ_2, respectively, and lose their infection ability at rate μ_U. Berries are produced by all types of mature leaves at rates $\delta_S \geq \delta_L \geq \delta_I \geq \delta_R$ and die at rate μ_B.

Table 1 summarises the parameter definitions and values of system (1).

Table 1 Description and values of parameters for system (1)

Symbol	Biological meaning	Value	Source
r_0	Production rate of J_S	2 /day	Assumed
r_1	Competition rate	0.02 /leaf.day	Assumed
ε	Infection-related production ratio	0.06	Assumed
ω_1	Germination rate on J_S	0.055 leaves/spore	ref[1]
ω_2	Germination rate on M_S	0.065 leaves/spore	ref[1]
γ_1	Sporulation rate by J_I	5 spores/leaf.day	ref[2]
γ_2	Sporulation rate by M_I	7 spores/leaf.day	ref[2]
ν	Deposition rate	0.09 /day	ref[2]
β	Maturation rate	0.05 /day	Assumed
θ	1 / duration of latency period	0.033 /day	ref[3]
α	1 / duration of sporulation period	0.066 /day	Assumed
μ_J	Mortality rate of J	0.0054 /day	Assumed
μ_M	Mortality rate of M	0.0034 /day	Assumed
μ_U	Mortality rate of U	0.035 /day	ref[4]
d	Extra mortality rate of M_R	0.056 /day	Assumed
δ_S	Berry production rate by M_S	0.7 berries/leaf.day	ref[5]
δ_L	Berry production rate by M_L	0.5 berries/leaf.day	ref[5]
δ_I	Berry production rate by M_I	0.3 berries/leaf.day	ref[5]
δ_R	Berry production rate by M_R	0.05 berries/leaf.day	ref[5]
μ_B	Mortality rate of B	0.0021 /day	Assumed

ref[1]: (Rayner, 1961), ref[2]: (Bock, 1962), ref[3]: (Waller, 1982), ref[4]: (Zambolim, 2016) and ref[5]: (Charrier and Berthaud, 1985).

From the compartmental model in Figure 1, we have the following system of ordinary differential equations:

$$\begin{cases} \dot{J}_S &= r_0 M_1 - r_1 M J_S - \frac{\omega_1 \nu U}{J+M} J_S - (\beta + \mu_J) J_S, \\ \dot{J}_L &= \frac{\omega_1 \nu U}{J+M} J_S - (\beta + \theta + \mu_J) J_L, \\ \dot{J}_I &= \theta J_L - (\beta + \alpha + \mu_J) J_I, \\ \dot{M}_S &= \beta J_S - \frac{\omega_2 \nu U}{J+M} M_S - \mu_M M_S, \\ \dot{M}_L &= \beta J_L + \frac{\omega_2 \nu U}{J+M} M_S - (\theta + \mu_M) M_L, \\ \dot{M}_I &= \beta J_I + \theta M_L - (\alpha + \mu_M) M_I, \\ \dot{M}_R &= \alpha M_I - (\mu_M + d) M_R, \\ \dot{U} &= \gamma_1 J_I + \gamma_2 M_I - (\nu + \mu_U) U. \\ \dot{B} &= \delta_1 M_S + \delta_2 M_L + \delta_3 M_I + \delta_4 M_R - \mu_B B, \end{cases} \tag{1}$$

Since B is not present in the other equations of system (1), we do not consider this state variable in the mathematical analysis. With this in mind, system (1) reduces to

$$\begin{cases} \dot{J}_S &= r_0 M_1 - r_1 M J_S - \frac{\omega_1 \nu U}{J+M} J_S - (\beta + \mu_J) J_S, \\ \dot{J}_L &= \frac{\omega_1 \nu U}{J+M} J_S - k_1 J_L, \\ \dot{J}_I &= \theta J_L - k_2 J_I, \\ \dot{M}_S &= \beta J_S - \frac{\omega_2 \nu U}{J+M} M_S - \mu_M M_S, \\ \dot{M}_L &= \beta J_L + \frac{\omega_2 \nu U}{J+M} M_S - k_3 M_L, \\ \dot{M}_I &= \beta J_I + \theta M_L - k_4 M_I, \\ \dot{M}_R &= \alpha M_I - k_5 M_R, \\ \dot{U} &= \gamma_1 J_I + \gamma_2 M_I - k_6 U. \end{cases} \tag{2}$$

where

$$k_1 = \beta + \theta + \mu_J, \quad k_2 = \beta + \alpha + \mu_J, \quad k_3 = \theta + \mu_M,$$
$$k_4 = \alpha + \mu_M, \quad k_5 = \mu_M + d, \quad k_6 = \nu + \mu_U,$$

System (2) is not defined when $J + M = 0$, so we need to consider the following domain for the well-posedness of the system

$$\Gamma = \mathbb{R}^8_+ \setminus \{(0, 0, 0, 0, 0, 0, 0, U) \text{ with } U \geq 0\}$$

where $\mathbb{R}_+$ is the set of non-negative real numbers.

2.2 Basic properties

We obtain the following results for the non-negativity and boundedness of solutions of system (2).

Lemma 1 *For any initial condition in* Γ*, system* (2) *has a unique local non-negative solution in* Γ.

Proof : Let $x = (J_S, J_L, J_I, M_S, M_L, M_I, M_R, U)$ and $x(0)$ be an initial condition in Γ of system (2).

Suppose that one of the variables, that we will denote x_i is equal to 0 at some time, with all others being non-negative. A quick analysis shows that $\dot{x}_i \geq 0$ so that x_i cannot become negative Farina and Rinaldi (2000). To ensure that the solution exist in Γ, we still need to prove that $J + M$ cannot become zero in finite time.

Using system (2), we obtain

$$\begin{aligned} \dot{J} + \dot{M} &= r_0 M_1 - r_1 M J_S - \mu_J J - \mu_M M - \alpha J_I - d M_R, \\ &\geq -r_1 M J_S - \mu_J J - \mu_M M - \alpha J_I - d M_R. \end{aligned}$$

Using the fact that $J_S < J < J + M$, $M < J + M$, $J_I < J + M$ and $M_R < J + M$, one has

$$\widehat{J + M} \geq -r_1 (J + M)^2 - \Upsilon (J + M) \tag{3}$$

where $\Upsilon = \mu_J + \mu_M + \alpha + d$. Using the comparison theorem to solve inequation (3) yields

$$J(t) + M(t) \geq \frac{\Upsilon (J(0) + M(0))}{\Upsilon e^{\Upsilon t} + (J(0) + M(0))(e^{\Upsilon t} - 1)}.$$

The above expression proves that $J(t)+M(t)$ cannot reach 0 in finite time. Therefore, the right hand-side of system (2) is Lipschitz continuous along all solutions, which implies that this system admits a unique solution that stays in Γ at all time.

□

We also obtain the following result about the boundedness of solutions of system (2).

Lemma 2 *All solutions of system (2) are bounded.*

Proof :

For any given initial conditions, let us choose $U_{\max}$ large enough i.e

$$U_{\max} \geq \max\left\{ \frac{J_L(0)^2}{\mathcal{K}_{J_L}^2}, \frac{J_I(0)^2}{\mathcal{K}_{J_I}^2}, \frac{M_L(0)^2}{\mathcal{K}_{M_L}^2}, \frac{M_I0)^2}{\mathcal{K}_{M_I}^2}, \frac{M_R(0)^2}{\mathcal{K}_{M_R}^2}, \mathcal{K}_U \right\}.$$

where

$$\overline{J_S} = \max(J_S(0), \frac{r_0}{r_1}), \quad \overline{M_S} = \max\left(M_S(0), \frac{\beta}{\mu_M}\overline{J_S}\right), \quad \mathcal{K}_{J_L} = \sqrt{\frac{\omega_1 \nu \overline{J_S}}{k_1}},$$

$$\mathcal{K}_{J_I} = \frac{\theta \mathcal{K}_{J_L}}{k_2} \quad \mathcal{T}_1 = \sqrt{\beta^2 \mathcal{K}_{J_L}^2 + 4k_3\omega_2\nu\overline{M_S}}, \quad \mathcal{K}_{M_L} = \frac{\beta \mathcal{K}_{J_L} + \mathcal{T}_1}{2k_3},$$

$$\mathcal{K}_{M_I} = \frac{\beta \mathcal{K}_{J_L} + \theta \mathcal{K}_{M_L}}{k_4}, \quad \mathcal{K}_{M_R} = \frac{\alpha \mathcal{K}_{M_I}}{k_5} \quad \mathcal{T}_2 = \gamma_1 \mathcal{K}_{J_I} + \gamma_2 \mathcal{K}_{M_I}, \text{ and } \mathcal{K}_U = \frac{\mathcal{T}_2^2}{k_6^2}.$$

To prove the boundedness of solutions, let us prove that the compact region given by

$$\Omega = \left\{ \begin{array}{l} (J_S, J_L, J_I, M_S, M_L, M_I, M_R, U) \in \mathbb{R}_+^8, J_S \leq \overline{J_S}, J_L \leq \mathcal{K}_{J_L}\sqrt{U_{\max}}, \\ J_I \leq \mathcal{K}_{J_I}\sqrt{U_{\max}}, M_S \leq \overline{M_S}, M_L \leq \mathcal{K}_{M_L}\sqrt{U_{\max}}, M_I \leq \mathcal{K}_{M_I}\sqrt{U_{\max}}, \\ M_R \leq \mathcal{K}_{M_R}\sqrt{U_{\max}} \quad \text{and} \quad U \leq U_{\max}, \text{with} \quad U_{\max} \geq \mathcal{K}_U \end{array} \right\},$$

is positively invariant for system (2).

Consider the first equation of system (2):

$$\dot{J}_S = r_0 M_1 - r_1 M J_S - \frac{\omega_1 \nu U}{J+M} J_S - (\beta + \mu_J) J_S.$$

Using the fact that $\frac{\omega_1 \nu U}{J+M} J_S \geq 0$ and $M_1 \leq M$, we obtain the following equation

$$\dot{J}_S \leq r_0 M \left(1 - \frac{J_S}{\frac{r_0}{r_1}}\right) - (\beta + \mu_J) J_S.$$

If $J_S(0) \geq r_0/r_1$, then $\dot{J}_S(t) \leq 0$, which implies that $\forall t\ J_S(t) \leq J_S(0) = \max(J_S(0), r_0/r_1)$. If $J_S(0) \leq r_0/r_1$, then $\dot{J}_S(t) \leq 0$ when $J_S(t) = r_0/r_1$, which implies that $\forall t\ J_S(t) \leq r_0/r_1 = \max(J_S(0), r_0/r_1)$. Then one can conclude that $\forall t\ J_S(t) \leq \bar{J}_S = \max(J_S(0), r_0/r_1)$

Similarly, let us consider the fourth equation of system (2).

$$\dot{M}_S = \beta J_S - \frac{\omega_2 \nu U}{J+M} M_S - \mu_M M_S,$$

Using the fact that $\frac{\omega_2 \nu U}{J+M} M_S \geq 0$ and $J_S \leq \overline{J_S}$, we obtain

$$\dot{M}_S \leq \beta \overline{J_S} - \mu_M M_S.$$

If $M_S \geq \frac{\beta}{\mu_M}\overline{J_S}$, one has $\dot{M}_S \leq 0$, this allows to conclude for all $t \geq 0$ and $M_S(t) \leq \overline{M_S}$.

Now for the boundness of the other variables, we use the hypothesis that $\forall t \geq 0$, $U(t) \leq U_{\max}$ whose validity will be confirmed later. Let us consider the second equation of system (2):

$$\dot{J}_L = \frac{\omega_1 \nu U}{J+M} J_S - k_1 J_L$$

Using the fact that $\frac{J_S}{J+M} \leq \frac{\overline{J_S}}{J_L}$ and $U \leq U_{\max}$, we obtain

$$\dot{J}_L \leq \frac{\omega_1 \nu U_{\max} \overline{J_S}}{J_L} - k_1 J_L. \tag{4}$$

If $J_L \geq \mathcal{K}_{J_L}\sqrt{U_{\max}}$ in the equation (4) we obtain $\dot{J}_L \leq 0$. This implies that, if $J_L(0) \leq \mathcal{K}_{J_L}\sqrt{U_{\max}}$, then $J_L(t) \leq \mathcal{K}_{J_L}\sqrt{U_{\max}}$, for all $t \geq 0$.

Now, replacing the upper-bound value of J_L into the third equation of system (2), gives

$$\dot{J}_I \leq \theta \mathcal{K}_{J_L}\sqrt{U_{\max}} - k_2 J_I. \tag{5}$$

In the equation (5), one can observe that if $J_I \geq \mathcal{K}_{J_I}\sqrt{U_{\max}}$, we have $\dot{J}_I \leq 0$ so that, when $J_I(0) \leq \mathcal{K}_{J_I}\sqrt{U_{\max}} = \frac{\theta \mathcal{K}_{J_L}}{k_2}\sqrt{U_{\max}}$, we obtain $J_I(t) \leq \mathcal{K}_{J_I}\sqrt{U_{\max}}$, for all $t \geq 0$.

Replacing the upper-bound of J_L and U into the fifth equation of system (2) and using the fact $\frac{M_S}{J+M} \leq \frac{\overline{M_S}}{M_L}$, yields

$$\begin{aligned} \dot{M}_L &\leq \beta \mathcal{K}_{J_L}\sqrt{U_{\max}} + \frac{\omega_2 \nu U_{\max} \overline{M_S}}{M_L} - (\theta + \mu_M) M_L \\ &= \frac{-k_3 M_L^2 + \beta \mathcal{K}_{J_L}\sqrt{U_{\max}} M_L + \omega_2 \nu U_{\max} \overline{M_S}}{M_L}. \end{aligned} \tag{6}$$

The sign of the right-hand side of equation (6) is given by the sign of the second order equation of the numerator. Hence, it is negative when M_L is larger than the largest of its two roots. This largest root is given by $\mathcal{K}_{M_L}\sqrt{U_{\max}} = \frac{\beta \mathcal{K}_{J_L} + \mathcal{T}_1}{2k_3}\sqrt{U_{\max}}$. Then, one can conclude that when $M_L(0) \leq \mathcal{K}_{M_L}\sqrt{U_{\max}}$, one has $M_L(t) \leq \mathcal{K}_{M_L}\sqrt{U_{\max}}$ for all $t \geq 0$.

Replacing the upper-bound of J_I and M_L into sixth equation of system (2), gives

$$\dot{M}_I \leq \beta \mathcal{K}_{J_L}\sqrt{U_{\max}} + \theta \mathcal{K}_{M_L}\sqrt{U_{\max}} - k_4 M_I. \tag{7}$$

In the equation (7), one can observe that if $M_I \geq \mathcal{K}_{M_I}\sqrt{U_{\max}} = \frac{\beta \mathcal{K}_{J_L} + \theta \mathcal{K}_{M_L}}{k_4}\sqrt{U_{\max}}$, we have $\dot{M}_I \leq 0$ so that, when $M_I(0) \leq \mathcal{K}_{M_I}\sqrt{U_{\max}}$, we obtain $M_I(t) \leq \mathcal{K}_{M_I}\sqrt{U_{\max}}$, for all $t \geq 0$.

Replacing the upper-bound value of M_I into the seventh equation of system (2), yields

$$\dot{M}_R \leq \alpha \mathcal{K}_{M_I}\sqrt{U_{\max}} - k_5 M_R. \tag{8}$$

Thus, if $M_R \geq \mathcal{K}_{M_R}\sqrt{U_{\max}} = \frac{\alpha \mathcal{K}_{M_I}}{k_5}\sqrt{U_{\max}}$ in the equation (8) we obtain $\dot{M}_R \leq 0$, this implies, if $M_R(0) \leq \mathcal{K}_{M_R}\sqrt{U_{\max}}$, then $M_R(t) \leq \mathcal{K}_{M_R}\sqrt{U_{\max}}$, for all $t \geq 0$.

Replacing the upper-bound value of J_I and M_I into the eighth equation of system (2), gives

$$\dot{U} \leq \gamma_1 \mathcal{K}_{J_I} \sqrt{U_{\max}} + \gamma_2 \mathcal{K}_{M_I} \sqrt{U_{\max}} - k_6 U. \tag{9}$$

Let $\mathcal{T}_2 = \gamma_1 \mathcal{K}_{J_I} + \gamma_2 \mathcal{K}_{M_I}$, from the equation (9), one can observe that if $U \geq \frac{\mathcal{T}_2}{k_6} \sqrt{U_{\max}}$, we obtain $\dot{U} \leq 0$. Thus, as $U_{\max} \geq \mathcal{K}_U = \frac{\mathcal{T}_2^2}{k_6^2}$, we obtain $\dot{U} \leq 0$ for $U = U_{max}$. Hence, the positive invariance of Ω is shown.

□

Theorem 3 *For any initial condition in Ω, system (2) has a unique global solution in Ω.*

Proof Lemma 1 and Lemma 2 allow to conclude the existence and uniqueness of bounded global non-negative solution of system (2) defined on Γ. □

Remark 1 System (2) is not defined for $(J_S, J_L, J_I, M_S, M_L, M_I, M_R) = 0_{\mathbb{R}^7}$ but is extended to the trivial equilibrium $0_{\mathbb{R}^8}$ which makes sense biologically. However, the stability of this trivial equilibrium cannot be analysed as the Jacobian matrix of system (2) is not defined at this point.

3 The disease free equilibrium and its stability

The disease free equilibrium (DFE) of system (2) occurs in the absence of CLR, so the DFE is

$$x^1 = (J_S^1, 0, 0, M_S^1, 0, 0, 0, 0)$$

where

$$J_S^1 = \frac{r_0\beta - \mu_M(\beta + \mu_J)}{\beta r_1} \qquad \text{and} \qquad M_S^1 = \frac{\beta J_S^1}{\mu_M}. \tag{10}$$

The above expression shows that the DFE exists under the following condition:

$$r_0\beta - \mu_M(\beta + \mu_J) > 0. \tag{11}$$

If condition (11) does not hold, the plantation of coffee cannot survive.

3.1 The basic reproduction number and the local stability of the DFE

We have the following result about the local stability of the DFE.

Lemma 4 *The DFE x^1 of system (2) is locally asymptotically stable (LAS) in Γ when $\mathcal{R}_0 < 1$, and unstable if $\mathcal{R}_0 > 1$.*

Proof : Let us compute the basic reproduction number for the local stability of the DFE of system (2). To do so, we use the standard method of the next generation matrix developed by (Van den Driessche and Watmough, 2002). In system (2), we consider only the variables in which the infection is in progression and uredospores, i.e. J_L, J_I, M_L, M_I, M_R and U. The corresponding equations can be rewritten in the following way

$$\frac{dx_I}{dt} = \mathcal{F}(x) - \mathcal{V}(x),$$

where $x_I = (J_L, J_I, M_L, M_I, M_R, U)$, $\mathcal{F}_i(x)$ represents the rate of appearance of the new infections in compartment i and $V(x)$ the transfer terms between compartments or the outside. We have

$$\mathcal{F}(x) = \begin{pmatrix} \frac{\omega_1 \nu U}{J+M} J_S \\ 0 \\ \frac{\omega_2 \nu U}{J+M} M_S \\ 0 \\ 0 \\ 0 \end{pmatrix} \quad \text{and} \quad \mathcal{V}(x) = \begin{pmatrix} k_1 J_L \\ -\theta J_L + k_2 J_I \\ -\beta J_L + k_3 M_L \\ -\beta J_I - \theta M_L + k_4 M_I \\ -\alpha M_I + k_5 M_R \\ -\gamma_1 J_I - \gamma_2 M_I + k_6 U \end{pmatrix}.$$

The Jacobian matrices F of $\mathcal{F}$ and V of $\mathcal{V}$ evaluated at the DFE x^1 are respectively

$$F = \begin{pmatrix} 0 & 0 & 0 & 0 & 0 & \frac{\omega_1 \nu J_S^1}{J_S^1 + M_S^1} \\ 0 & 0 & 0 & 0 & 0 & 0 \\ 0 & 0 & 0 & 0 & 0 & \frac{\omega_2 \nu M_S^1}{J_S^1 + M_S^1} \\ 0 & 0 & 0 & 0 & 0 & 0 \\ 0 & 0 & 0 & 0 & 0 & 0 \\ 0 & 0 & 0 & 0 & 0 & 0 \end{pmatrix} \quad \text{and} \quad V = \begin{pmatrix} k_1 & 0 & 0 & 0 & 0 & 0 \\ -\theta & k_2 & 0 & 0 & 0 & 0 \\ -\beta & 0 & k_3 & 0 & 0 & 0 \\ 0 & -\beta & -\theta & k_4 & 0 & 0 \\ 0 & 0 & 0 & -\alpha & k_5 & 0 \\ 0 & -\gamma_1 & 0 & -\gamma_2 & 0 & k_6 \end{pmatrix}.$$

The basic reproduction number $\mathcal{R}_0$ is obtained as the spectral radius of the positive matrix FV^{-1}, that is

$$\mathcal{R}_0 = \frac{\nu\theta \left[\omega_1 \mu_M [\beta\gamma_2(k_2 + k_3) + \gamma_1 k_3 k_4] + \beta\omega_2\gamma_2 k_1 k_2\right]}{k_1 k_2 k_3 k_4 k_6 (\beta + \mu_M)}. \tag{12}$$

□

3.2 Global stability of DFE

Using a result obtained by Kamgang and Sallet (Kamgang, 2003), we have the following result about the global stability of the DFE.

Theorem 5 *If* $\mathcal{R}_0 \leq \xi < 1$, *where*

$$\xi = \frac{\mu_M}{\beta + \mu_M} \left(1 + \frac{\nu\theta\omega_2\gamma_2}{k_3 k_4 k_6} \left(\frac{\beta}{\mu_M} - 1\right)\right),$$

then the DFE x^1 *of system (2) is globally asymptotically stable (GAS) in* Γ.

Proof : For the proof of this global stability, using the property of DFE, we rewrite system (2) in the following compact form

$$\begin{cases} \dot{x}_S = G_{11}(x_S, x_I)(x_S - x_S^1) - G_{12}(x_S, x_I)x_I \\ \dot{x}_I = G_{22}(x_S, x_I)x_I \end{cases} \tag{13}$$

where x_S is the vector representing the state of different compartments of non-transmitting leaves (e.g. susceptible leaves) and the vector x_I represents the state of compartments of different transmitting leaves (e.g. infected leaves). Here, we have $x_S = (J_S, M_S)^T$, $x_I = (J_L, J_I, M_L, M_I, M_R, U)^T$, $x_S^1 = (J_S^1, M_S^1)^T$, $x = (x_S, x_I)$,

$$G_{11}(x_S, x_I) = \begin{pmatrix} -r_1 M - (\beta + \mu_J) & r_0 - r_1 J_S^1 \\ \beta & -\mu_M \end{pmatrix},$$

$$G_{12}(x_S, x_I) = \begin{pmatrix} 0 & 0 & r_0 - r_1 J_S^1 & \varepsilon r_0 - r_1 J_S^1 & \varepsilon r_0 - r_1 J_S^1 & -\frac{\omega_1 \nu J_S}{J+M} \\ 0 & 0 & 0 & 0 & 0 & -\frac{\omega_2 \nu M_S}{J+M} \end{pmatrix}$$

and

$$G_{22}(x_S, x_I) = \begin{pmatrix} -k_1 & 0 & 0 & 0 & 0 & \frac{\omega_1 \nu J_S}{J+M} \\ \theta & -k_2 & 0 & 0 & 0 & 0 \\ \beta & 0 & -k_3 & 0 & 0 & \frac{\omega_2 \nu M_S}{J+M} \\ 0 & \beta & \theta & -k_4 & 0 & 0 \\ 0 & 0 & 0 & \alpha & -k_5 & 0 \\ 0 & \gamma_1 & 0 & \gamma_2 & 0 & -k_6 \end{pmatrix}.$$

Let $\Omega \subset \mathcal{U} = \mathbb{R}_+^2 \times \mathbb{R}_+^6$. The right-hand side of system (13) is of class C^1 on the open set $\mathcal{U}$. Let us verify the following five hypotheses for the application of the Kamgang and Sallet's theorem.

H_1: System (13) is defined on a positively invariant set Ω of the nonnegative orthant. System (13) is dissipative on Ω

H_2: Subsystem $\dot{x}_I = G_{11}(x_S, 0)(x_S - x_S^1)$ is globally asymptotically stable at the equilibrium $x_S^1 = (J_S^1, M_S^1)$ on the canonical projection $\mathfrak{D} = \Omega \cap (\mathbb{R}_+^2 \times \{0_{\mathbb{R}^6}\})$ of Ω on $\mathbb{R}_+^2$

Indeed, this subsystem can be written as

$$\begin{cases} \frac{dJ_S(t)}{dt} = r_0 M_S - r_1 J_S M_S - (\beta + \mu_J) J_S, \\ \frac{dM_S(t)}{dt} = \beta J_S - \mu_M M_S \end{cases} \tag{14}$$

System (14) has two equilibria: a trivial equilibrium which is unstable and the DFE $x_S^1 = (J_S^1, M_S^1)$, (where the values of J_S^1 and M_S^1 are given above and exist under condition (11)) which is globally asymptotically stable.

H_3: Matrix $G_{22}(x_S, x_I)$ is Metzler and irreducible for any given $x \in \Omega$.

H_4: There exists an upper-bound matrix $\hat{G}_{22}$ for $\mathfrak{M} = \{G_{22}(x) \in \mathcal{M}_6(\mathbb{R}) / x \in \Omega\}$ with the property that either $\hat{G}_{22} \notin \mathfrak{M}$ or if $\hat{G}_{22} \in \mathfrak{M}$, (i.e., $\hat{G}_{22} = \max_\Omega \mathfrak{M}$), then for any $\bar{x} \in \Omega$ such that $\hat{G}_{22} = G_{22}(\bar{x})$, $\bar{x} \in \mathbb{R}_+^2 \times \{0\}$.

Indeed, consider the subsystem $\dot{x}_I = G_{22}(x_S, x_I)x_I$, on the matrix $G_{22}(x)$, we have $\frac{J_S}{J+M} \leq 1$ and $\frac{M_S}{J+M} \leq 1$, this implies that $\dot{x}_I \leq \hat{G}_{22} x_I$, where $\hat{G}_{22}$

can be written as $\hat{G}_{22} = \hat{F} - V$, with V given above and

$$\hat{F} = \begin{pmatrix} 0 & 0 & 0 & 0 & 0 & \omega_1\nu \\ 0 & 0 & 0 & 0 & 0 & 0 \\ 0 & 0 & 0 & 0 & 0 & \omega_2\nu \\ 0 & 0 & 0 & 0 & 0 & 0 \\ 0 & 0 & 0 & 0 & 0 & 0 \\ 0 & 0 & 0 & 0 & 0 & 0 \end{pmatrix}.$$

H_5: The spectral radius of the matrix $\hat{G}_{22}$ verifies $\sigma(\hat{G}_{22}) \leq 0$.

Indeed, consider the following auxiliary problem:

$$\frac{d\hat{x}_I}{dt} = (\hat{F} - V)\hat{x}_I. \tag{15}$$

The matrix $\hat{F}$ and V verify the condition of Theorem 2 in (Van den Driessche and Watmough, 2002), then we have $\sigma(\hat{G}_{22}) = \sigma(\hat{F} - V) < 0$, which implies that $\mathcal{R}_C = \sigma(\hat{F}V^{-1}) \leq 1$, where $\sigma(\hat{F} - V)$ represents the spectral radius of the matrix $\hat{F} - V$ (i.e. the largest real part of all the eigenvalues of this matrix) and $\hat{F}V^{-1}$ is the next generation matrix. The computation gives

$$\mathcal{R}_C = \frac{\nu\theta\left[\omega_1[\beta\gamma_2(k_2 + k_3) + \gamma_1 k_3 k_4] + \omega_2\gamma_2 k_1 k_2\right]}{k_1 k_2 k_3 k_4 k_6}.$$

Thus $\mathcal{R}_C \leq 1$ ensures that all eigenvalues of $\hat{G}_{22}$ have a negative real parts. We have computed $\mathcal{R}_C$ and we have seen that the hypotheses H_1, H_2 , H_3 , H_4 and H_5 are satisfied. Then, by Kamgang and Sallet (2008), we have proven that the DFE x^1 for the system (2) is GAS if $\mathcal{R}_C \leq 1$.

One can observe that

$$\mathcal{R}_0 = \frac{\mu_M}{\beta + \mu_M}\left(\mathcal{R}_C + \frac{\nu\theta\omega_2\gamma_2}{k_3 k_4 k_6}\left(\frac{\beta}{\mu_M} - 1\right)\right),$$

so that $\mathcal{R}_C \leq 1$ if and only if

$$\mathcal{R}_0 \leq \xi,$$

where

$$\xi = \frac{\mu_M}{\beta + \mu_M}\left(1 + \frac{\nu\theta\omega_2\gamma_2}{k_3 k_4 k_6}\left(\frac{\beta}{\mu_M} - 1\right)\right). \tag{16}$$

Then, Lemma 4 and hypothesis $H_1 - H_5$ allow to conclude that the DFE is GAS if $\mathcal{R}_0 \leq \xi < 1$, where ξ is given above. This completes the proof. □

4 Endemic equilibria and their stability

Herein we prove the existence of endemic equilibria (EE) of system (2) and analyse their stability.

Proposition 1 (Existence of endemic equilibria) *We denote by λ the force of infection given by*

$$\lambda = \frac{\nu U}{J + M}. \tag{17}$$

Let $x^* = (J_S^*, J_L^*, J_I^*, M_S^*, M_S^*, M_L^*, M_I^*, M_R^*, U^*)$ *be an endemic equilibrium of system* (2). *Setting the right hand side of this system to* 0 *yields*

$$\begin{cases} 0 = r_0 M_1^* - r_1 M^* J_S^* - \omega_1 \lambda^* J_S^* - (\beta + \mu_J) J_S^* \\ J_L^* = \lambda^* \dfrac{\omega_1}{k_1} J_S^*, \\ J_I^* = \lambda^* \dfrac{\theta \omega_1}{k_1 k_2} J_S^*, \\ M_S^* = \dfrac{\beta J_S^*}{(\mu_M + \lambda^* \omega_2)}, \\ M_L^* = \lambda^* \left(\dfrac{\beta \omega_1}{k_1 k_3} J_S^* + \dfrac{\omega_2}{k_3} M_S^* \right), \\ M_I^* = \lambda^* \left(\dfrac{\beta \theta \omega_1 (k_2 + k_3)}{k_1 k_2 k_3 k_4} J_S^* + \dfrac{\theta \omega_2}{k_3 k_4} M_S^* \right), \\ M_R^* = \lambda^* \left(\dfrac{\beta \theta \alpha \omega_1 (k_2 + k_3)}{k_1 k_2 k_3 k_4 k_5} J_S^* + \dfrac{\theta \alpha \omega_2}{k_3 k_4 k_5} M_S^* \right), \\ U^* = \lambda^* \left(\dfrac{\theta \omega_1 (\beta \gamma_2 (k_2 + k_3) + \gamma_1 k_3 k_4)}{k_1 k_2 k_3 k_4 k_6} J_S^* + \dfrac{\theta \gamma_2 \omega_2}{k_3 k_4 k_6} M_S^* \right). \end{cases} \tag{18}$$

One can observe that there exists an endemic equilibrium x^* *if and only if* λ^* *and* J_S^* *are positive.*

Substituting the expressions of $J^*_{\{L,I\}}$ *and* $M^*_{\{S,L,I,R\}}$ *into the first equation of system* (18) *and solving this equation for* J_S^*, *we obtain either* $J_S^* = 0$ *which corresponds to the trivial equilibrium or*

$$J_S^* = \frac{b_2 (\lambda^*)^2 + b_1 \lambda^* + b_0}{\beta r_1 (c_2 (\lambda^*)^2 + c_1 \lambda^* + c_0)}, \tag{19}$$

where

$$\begin{cases} b_2 = \omega_1 \omega_2 (\beta r_0 (\theta \varepsilon (\alpha + k_5)(k_2 + k_3) + k_2 k_4 k_5) - k_1 k_2 k_3 k_4 k_5), \\ b_1 = \beta r_0 k_2 \left[(k_5 (\varepsilon \theta + k_4) + \varepsilon \theta \alpha)(k_1 \omega_2 + \mu_M \omega_1) \right] + \beta r_0 \mu_M \theta \varepsilon \omega_1 k_3 (\alpha + k_5), \\ \qquad - k_1 k_2 k_3 k_4 k_5 (\omega_2 (\beta + \mu_J) + \mu_M \omega_1), \\ b_0 = (\beta r_0 - \mu_M (\beta + \mu_J)) k_1 k_2 k_3 k_4 k_5, \\ c_2 = \omega_1 \omega_2 \left[\theta (k_2 + k_3)(\alpha + k_5) + k_2 k_4 k_5 \right], \\ c_1 = k_2 (k_1 \omega_2 + \mu_M \omega_1) \left[k_5 (\theta + k_4) + \alpha \theta \right] + \mu_M \theta \omega_1 k_3 (\alpha + k_5), \\ c_0 = k_1 k_2 k_3 k_4 k_5. \end{cases}$$

Note that, in the equation (19) *when* λ^* *is positive, the sign of* J_S^* *is determined by it numerator in* (19), *as all* $c_.$ *are positive.*

Let us study the positivity of the force of infection λ^*. *From equation (17) one has*

$$\lambda^* = \frac{\nu U^*}{J^* + M^*} \text{ implies } (J^* + M^*) = \frac{\nu U^*}{\lambda^*},$$

Replacing the expression of U^* *given in system* (18), *we obtain*

$$J^* + M^* = \nu \theta \left[\frac{\omega_1 [\beta \gamma_2 (k_2 + k_3) + \gamma_1 k_3 k_4]}{k_1 k_2 k_3 k_4 k_6} + \frac{\beta \omega_2 \gamma_2}{k_3 k_4 k_6 (\mu_M + \lambda^* \omega_2)} \right] J_S^*.$$

As $J^* + M^* = J_S^* + J_L^* + J_I^* + M_S^* + M_L^* + M_I^* + M_R^*$, *replacing the expressions given in equation* (18) *into the left-hand side of the above equation, we obtain either* $J_S^* = 0$ *or the following second degree polynomial:*

$$P(\lambda^*) = m_2 (\lambda^*)^2 + m_1 \lambda^* + m_0 \tag{20}$$

where

$$\begin{cases} m_2 = \omega_1\omega_2\left[\frac{\theta+k_2}{k_1k_2} + \frac{\beta}{k_1k_3} + \frac{\beta\theta(k_2+k_3)(\alpha+k_5)}{k_1k_2k_3k_4k_5}\right] \\ m_1 = \mu_M\frac{a_2}{\omega_2} + \omega_2\left[1 + \frac{\beta}{k_3} + \frac{\beta\theta(\alpha+k_5)}{k_3k_4k_5}\right] - \frac{\theta\omega_1\omega_2\nu[\beta\gamma_2(k_2+k_3)+\gamma_1k_3k_4]}{k_1k_2k_3k_4k_6} \\ m_0 = (\beta+\mu_M)(1-\mathcal{R}_0)\,. \end{cases}$$

Now, using the Descartes sign rules for λ-polynomial (20), the number of positive solutions is given in Table 2.

Table 2 Descartes rule for λ-polynomial (20).

m_2	m_1	m_0	$\mathcal{R}_0$	Number of positive solutions
+	+	+	$\mathcal{R}_0 < 1$	No solution
+	-	+	$\mathcal{R}_0 < 1$	No or two solutions
+	+	-	$\mathcal{R}_0 > 1$	One solution
+	-	-	$\mathcal{R}_0 > 1$	One solution

A positive value for λ^* is not sufficient to obtain an endemic equilibrium of system (2). We also need to verify if the corresponding value of J_S^*, determined from equation (19), is positive. If both λ^* and J_S^* are positive, according to system (18), all state variables are positive, so it corresponds to an endemic equilibrium.

To study the stability of the endemic equilibria around $\mathcal{R}_0$, we use Theorem 6 given in Appendix A. We first introduce a positive parameter η and set $\gamma_2 = \eta\gamma_1$. Then, used γ_1 as a bifurcation parameter, its variations will cover all $\mathcal{R}_0$ values. Indeed,

$$\frac{\mathcal{R}_0}{\gamma_1} = \frac{\nu\theta(\omega_1\mu_M(\beta\eta(k_2+k_3)+k_3k_4)+\beta\omega_2\eta k_1k_2)}{k_1k_2k_3k_4k_6(\beta+\mu_M)} := \frac{1}{\zeta} > 0. \tag{21}$$

We show in Appendix A that the direction of the bifurcation is determined by the sign of parameter a defined in equation (A4). Parameter values in Table 1, with $\eta = 7/5$, lead to $a < 0$ which corresponds to a forward bifurcation.

4.1 Forward bifurcation and stability

Using Maple to calculate the solutions of the λ-polynomial in equation (20), we obtain Table 3.

From Table 3, one can conclude that system (2) has one endemic equilibrium when $\mathcal{R}_0 > 1$ and that the DFE always exists.

According to the results in Appendix A, when the bifurcation parameter changes from $\gamma_1 < \zeta$ to $\gamma_1 > \zeta$, i.e. the basic reproduction number changes from $\mathcal{R}_0 < 1$ to $\mathcal{R}_0 > 1$, the DFE changes from LAS to unstable. Moreover, the endemic equilibrium $J_{S,1}^*$ in Table 3 appears and is locally asymptotically stable.

Table 3 Force of infection λ and susceptible young leaves J_S at equilibrium using parameter values in Table 1, except for bifurcation parameter γ_1 and $\gamma_2 = \eta\gamma_1$ with $\eta = 7/5$. Note that $\mathcal{R}_0 = 4$ corresponds to parameter values close to Table 1 ($\gamma_1 = 4.74$ instead of 5, $\gamma_2 = 6.64$ instead of 7).

	Equilibrium values for:	
	λ	J_S
$\mathcal{R}_0 = 0.8$	$\lambda_0 = 0$	$J_S^0 = 0$
		$J_S^1 = 99.81$
$\gamma_1 = 0.94$	$\lambda_1^* < 0$	$J_{S,1}^* < 0$
	$\lambda_2^* < 0$	$J_{S,2}^* < 0$
$\mathcal{R}_0 = 4$	$\lambda_0 = 0$	$J_S^0 = 0$
		$J_S^1 = 99.81$
$\gamma_1 = 4.74$	$\lambda_1^* = 1.27$	$J_{S,1}^* = 81.94$
	$\lambda_2^* < 0$	$J_{S,2}^* < 0$

To complement this analytical result, Figure 2 shows the existence of equilibria and their stability. The following initial conditions have been chosen to be

$$x(0) = \left\{ \begin{array}{l} J_S(0) = J_S^1,\ J_L(0) = J_I(0) = 0,\ M_S(0) = M_S^1, \\ M_L(0) = M_I(0) = M_R(0) = 0,\ U(0) = U_0 > 0\ , B(0) = 0 \end{array} \right\}. \quad (22)$$

They correspond to the DFE except for the initial presence of uredospores and absence of berries.

For $\mathcal{R}_0 = 0.8 < 1$ (black curves), subplot (a) shows that system (1) has two equilibria, the DFE which is stable and the trivial equilibrium which we showed to be unstable numerically; subplot (b) shows the convergence of susceptible young leaves to their DFE value J_S^1.

For $\mathcal{R}_0 = 4 > 1$ (orange curves), subplot (a) shows that system (1) has three equilibria: the trivial equilibrium which is unstable, the DFE which is unstable and the endemic equilibrium which is stable; subplot (b) shows the convergence of susceptible young leaves to their endemic equilibrium value $J_{S,1}^*$.

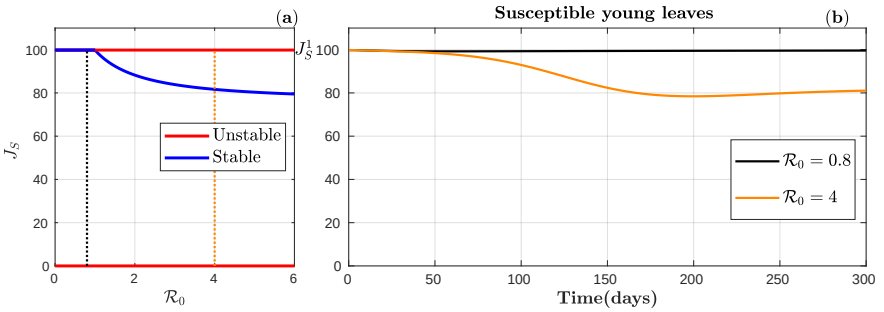

Fig. 2 Subplot (a) presents the $(\mathcal{R}_0, J_S)$-bifurcation diagram with stable (blue curve) and unstable (red curve) equilibria of system (1). Subplot (b) shows the dynamics of susceptible young leaves J_S for parameter values $\mathcal{R}_0 = 0.8$ (black curve) and $\mathcal{R}_0 = 4$ (orange curve) corresponding to the dotted lines in subplot (a). Bifurcation parameter is γ_1, $\mathcal{R}_0 = \gamma_1/\zeta$ and $\gamma_2 = \eta\gamma_1$, with ζ defined in equation (21) and $\eta = 7/5$. All remaining parameters are given in Table 1, leading to $\zeta = 1.185$ spores/leaf.day and initial conditions defined by (22) with $U_0 = 1000$ spores.

Figure 3 shows the convergence of system (1) towards the endemic equilibrium for different initial uredospore values. Susceptible leaves decrease over time. Infected leaves and uredospores overshoot their endemic steady state values. Compared to the DFE value ($B^1 = 48929$ berries), the number of berry at endemic equilibrium ($B^* = 8212$ berries) is drastically reduced by 83%.

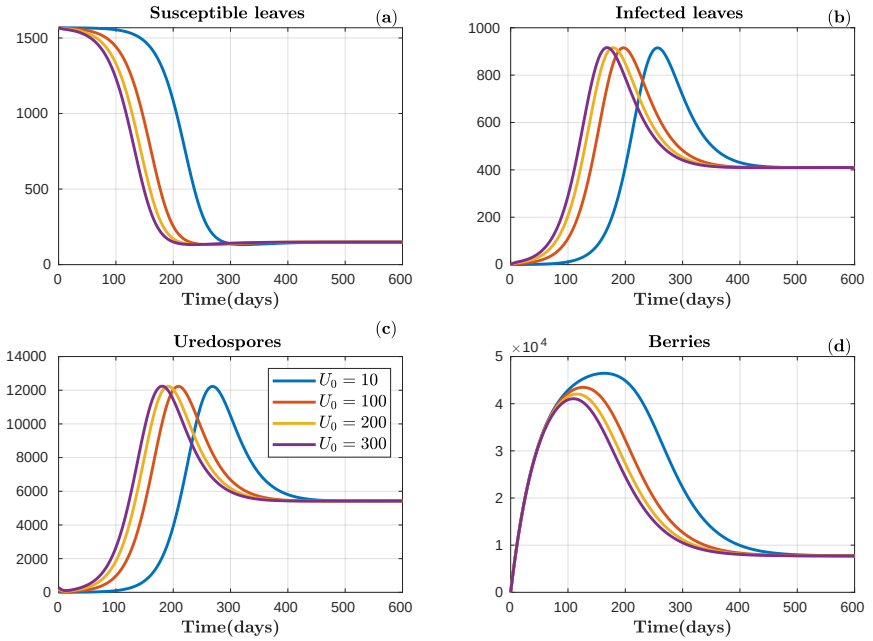

Fig. 3 Simulations of system (1) for $\mathcal{R}_0 = 4.218$, using initial conditions (22) with $U_0 = 10$ (blue curves), $U_0 = 100$ (red curves), $U_0 = 300$ (yellow curves) and $U(0) = 350$ spores (purple curves): (a) susceptible leaves $J_S + M_S$, (b) infected leaves $J_L + J_I + M_L + M_I + M_R$, (c) uredospores U and (d) berries B. All parameter values are given in Table 1.

4.2 Backward bifurcation and stability

In this subsection we study the behavior of system (1) when there is a backward bifurcation, corresponding to $a > 0$ in equation (A4). We choose ad hoc parameters given in Table 4.

Table 4 Parameter values of system (1) chosen to obtain a backward bifurcation.

Symbol	Value	Symbol	Value
r_0	0.7094 /day	θ	0.2336 /day
r_1	0.0065 /day	α	0.8261 /day
ω_1	0.4709 leaves/spore	μ_J	0.0114 /day
ω_2	0.5092 leaves/spore	μ_M	0.0236 /day
η	0.0396	μ_U	0.0931 /day
ν	0.6269 /day	d	0.0961 /day
β	0.0555 /day	ε	0.9953 /day

Firstly, using Maple to calculate the equilibria of system (2), we obtain Table 5. In this table, negative or complex values of λ^* and/or J_S^* are included (text in gray), but they do not correspond to biological equilibria.

From Table 5, we conclude that system (2) may have two endemic equilibria when $\mathcal{R}_0 < 1$ and has at most one endemic equilibrium when $\mathcal{R}_0 > 1$.

Table 5 Force of infection λ and susceptible young leaves J_S at equilibrium using parameter values in Table 4, with γ_1 the bifurcation parameter and $\gamma_2 = \eta\gamma_1$.

	Equilibrium values for:	
	λ	J_S
		$J_S^0 = 0$
$\mathcal{R}_0 = 0.3$	$\lambda_0 = 0$	$J_S^1 = 109.13$
$\gamma_1 = 2.33$	λ_1^* complex	$J_{S,1}^*$ complex
	λ_2^* complex	$J_{S,2}^*$ complex
		$J_S^0 = 0$
$\mathcal{R}_0 = 0.88$	$\lambda_0 = 0$	$J_S^1 = 109.13$
$\gamma_1 = 6.83$	$\lambda_1^* = 0.2$	$J_{S,1}^* = 88.82$
	$\lambda_2^* = 0.028$	$J_{S,2}^* = 102.07$
		$J_S^0 = 0$
$\mathcal{R}_0 = 4$	$\lambda_0^* = 0$	$J_S^1 = 109.13$
$\gamma_1 = 31.08$	$\lambda_1^* = 2.96$	$J_{S,1}^* = 58.54$
	$\lambda_2^* < 0$	$J_{S,2}^* < 0$

When $\mathcal{R}_0 < 1$, the DFE is stable. Moreover, according to the results in Appendix A, when $\mathcal{R}_0$ is close to one, there exist two endemic equilibria among which one is stable and the other unstable. When $\mathcal{R}_0 > 1$, the DFE is unstable. Moreover, when $\mathcal{R}_0$ is close to one, there is a unique endemic equilibrium, which is stable.

Figure 4 illustrates the existence of the endemic equilibria and their stability. The diagram in subplot (a) presents a sequence of two bifurcations: a saddle-node bifurcation in $\mathcal{R}_0 \approx 0.79$ and a backward transcritical bifurcation in $\mathcal{R}_0 = 1$. Subplot (b) presents the dynamics of susceptible young leaves J_S for representative parameter values.

For $\mathcal{R}_0 = 0.3$ (blue curves), subplot (a) shows that system (1) has two equilibria: the trivial equilibrium which we showed to be unstable numerically and the DFE which is stable; subplot (b) shows the convergence of susceptible young leaves to their DFE value J_S^1.

For $\mathcal{R}_0 = 0.88$ (black curves), subplot (a) shows that system (1) has four equilibria: the trivial equilibrium which is unstable, the DFE which is stable, the endemic equilibrium $J_{S,1}^*$ which is stable and the endemic equilibrium $J_{S,2}^*$ which is unstable; subplot (b) shows the convergence of susceptible young leaves to their DFE value J_S^1 (for $U_0 = 100$ spores) and to their endemic equilibrium value $J_{S,1}^*$ (for $U_0 = 1000$ spores).

For $\mathcal{R}_0 = 4$ (orange curves), subplot (a) shows that system (1) has three equilibria: the trivial equilibrium which is unstable, the DFE which is unstable and the endemic equilibrium which is stable; subplot (b) shows the convergence of susceptible young leaves to their endemic equilibrium value $J_{S,1}^*$.

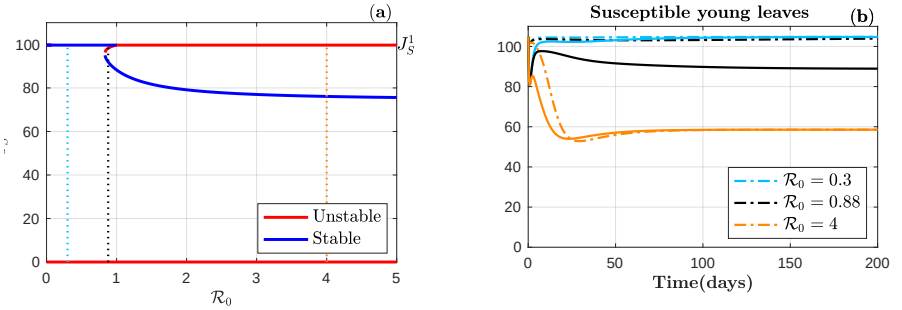

Fig. 4 Subplot (a) presents the $(\mathcal{R}_0, J_S)$-bifurcation diagram with stable (blue curve) and unstable (red curve) equilibria of system (1). Subplot (b) shows the dynamics of susceptible young leaves J_S for parameter values $\mathcal{R}_0 = 0.3$ (blue curves), $\mathcal{R}_0 = 0.88$ (black curves) and $\mathcal{R}_0 = 4$ (orange curves) corresponding to the dotted lines in subplot (a). The bifurcation parameter is γ_1, $\mathcal{R}_0 = \gamma_1/\zeta$ and $\gamma_2 = \eta\gamma_1$, with ζ defined in equation (21). All remaining parameters are given in Table 4, leading to $\zeta = 7.01$ spores/leaf.day and initial conditions defined by (22) with $U_0 = 100$ (dashed curves) and $U_0 = 1000$ spores (solid curves).

For $\mathcal{R}_0 = 0.88$, Figure 5 shows the convergence of system (1) towards the DFE and towards the stable endemic equilibrium for different initial uredospore values. For $U_0 = 10$ (blue curves) and $U_0 = 100$ spores (red curves), susceptible leaves decrease and then increase towards their DFE values. Simultaneously, the infected leaves and uredospores decrease towards zero and the berries increase. This convergence corresponds to the local stability of the DFE. For $U_0 = 400$ (yellow curves) and $U(0) = 500$ spores (purple curves), susceptible leaves decrease towards their endemic values. Infected leaves and uredospores first decrease, as for smaller initial uredospore values, and then increase towards their endemic values. Berries increase and then decrease towards their endemic values. This convergence corresponds to the local stability of one of the two endemic equilibria.

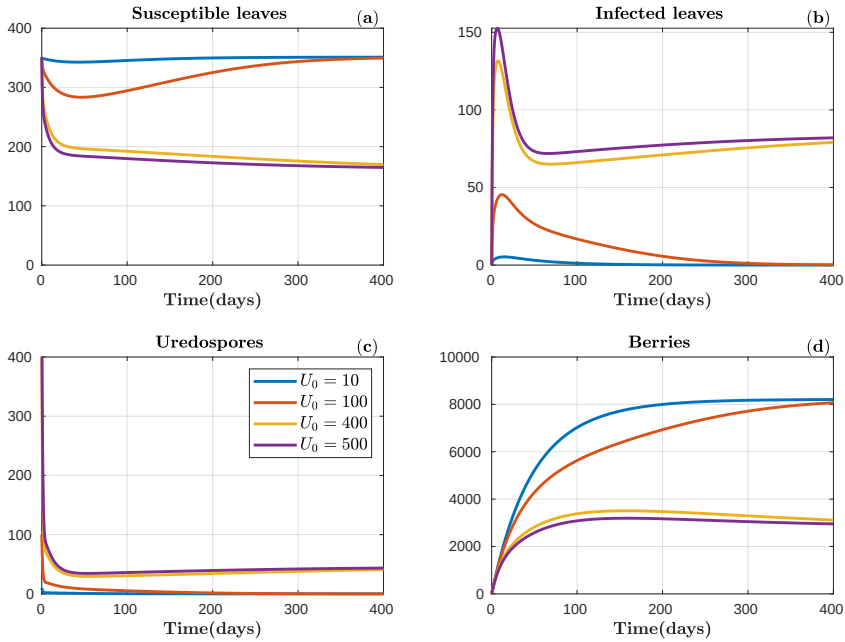

Fig. 5 Simulations of model (1) for $\mathcal{R}_0 = 0.8$, using initial conditions (22) with $U_0 = 10$ (blue curves), $U_0 = 100$ (red curves), $U_0 = 400$ (yellow curves) and $U(0) = 500$ spores (purple curves): (a) susceptible leaves $J_S + M_S$, (b) infected leaves $J_L + J_I + M_L + M_I + M_R$, (c) uredospores U and (d) berries B. All parameter values are given in Table 4 except $\gamma_1 = 6.18$ spores/leaf.day.

5 Discussion

In section 4, to determine the necessary and sufficient conditions for backward bifurcations in our model, which is structured in stages, we used the method proposed by Castillo-Chavez and Song (2004). Since our model remains a finite-dimensional system of differential equations, this approach was suitable. However, it is worth mentioning that Martcheva and Inaba (2020) extended the work of Castillo-Chavez and Song (2004) to models structured in age with infinite-dimensional characteristics, offering an alternative method for stability analysis. We have demonstrated that the high spore production by young leaves compared to mature leaves, leads to the occurrence of a backward bifurcation. This phenomenon, known as ontogenic resistance, is part of the various mechanisms identified by Gumel (2012); Inaba (2017) in their search for potential causes of bifurcation, in models related to human and animal epidemiology. To the best of our knowledge, the pioneering work by Gubbins et al (2000) marked the initial exploration of backward bifurcation in models concerning plant-parasite interactions. Subsequently, (Buonomo and Cerasuolo, 2014) conducted a study into the field of botanical epidemiology, where they

observed the occurrence of backward bifurcation. These two earlier studies did not consider age-structured models.

In human epidemiology, Zhang et al (2019) proposed a stage-structured epidemic model, where the disease can only be transmitted among adults. They proved that the model exhibits a backward bifurcation, which allows to conclude that ontogenic susceptibility may trigger backward bifurcation. However, in our paper, there is no backward bifurcation for ontogenic susceptibility, which is associated to the high infection risk of mature leaves.

6 Conclusion

In this paper, we proposed and analysed a mathematical model that describes the propagation of a fungal disease on a perennial plant. The originality of the model is the differentiation between young and mature leaves, to take into account the impact of host development on the aggressiveness of the pathogen. The model is applied to the particular case of coffee leaf rust in a coffee plantation. It is fairly generic and can be adapted to other fungal diseases for which the host age structure plays an important role.

We computed the disease-free and endemic equilibria and we studied their stability as a function of the basic reproduction number. We identified different bifurcation diagrams. They showed two behaviours for the model when the basic reproduction number is close to one, depending on the values of the sporulation rates in young and mature leaves. Ontogenic susceptibility on that trait yields a first case with a forward bifurcation, which corresponds to a stable disease free equilibrium when the basic reproduction number is less than one, and a stable endemic equilibrium when it is greater than one. Ontogenic resistance on that trait yields a second case with a backward bifurcation in which, on top of the stable disease free equilibrium, there is a stable endemic equilibrium when the basic reproduction number is less than one. This means that, disease may persist even in these unfavorable conditions. We illustrate in Appendix B two bifurcation cases that differ from the previous ones when the basic reproduction number is notably larger than one: the endemic equilibrium disappears and the trivial equilibrium becomes stable, which corresponds to the destruction of the plantation.

All bifurcation cases allow to conclude that, even when the basic reproduction number is less than one, the disease can persist. These results provide useful insights on the disease dynamics and its control. For instance, in order to eradicate a disease that spreads with basic reproduction number greater than one, it might not be sufficient to bring it below one, as an endemic state still persists. The basic reproduction number should be brought below the level of the saddle-node bifurcation to achieve effective disease control.

Conflict of interest

The authors declare that there are no conflicts of interest regarding the publication of this paper.

Code availability

The Matlab and Maple codes are available upon request.

Appendix A Bifurcation analysis

Theorem 6 (Castillo-Chavez and Song (Castillo-Chavez and Song, 2004)) *Consider the following ordinary differential equations, with a parameter ψ:*

$$\frac{dx}{dt} = f(x,\psi), \quad f : \mathbb{R}^n \times \mathbb{R} \to \mathbb{R}^n \quad \text{and} \quad f \in C^2(\mathbb{R}^n \times \mathbb{R}). \tag{A1}$$

Without loss of generality, it is assumed that 0 is an equilibrium for system (A1) for all values of the parameter ψ, that is $f(0,\psi) \equiv 0$ for all ψ. Assume

A_1: *$A = D_x f(0,0) = (\frac{\partial f_i}{\partial x_j}(0,0))$ is the linearization matrix of system (A1) around the equilibrium 0 with ψ evaluated at 0. Zero is a simple eigenvalue of A and all other eigenvalues of A have negative real parts;*

A_2: *Matrix A has a nonnegative right eigenvector u and a left eigenvector v corresponding to the zero eigenvalue. Let f_k be the k^{th} component of f and*

$$a = \sum_{k,i,j=1}^{n} v_k u_i u_j \frac{\partial^2 f_k}{\partial x_i \partial x_j}(0,0) \quad \text{and} \quad b = \sum_{k,i=1}^{n} v_k u_i \frac{\partial^2 f_k}{\partial x_i \partial \psi}(0,0).$$

The local dynamics of (A1) around 0 are totally determined by a and b.

1. *$a > 0$, $b > 0$. When $\psi < 0$ with $\|\psi\| \ll 1$, 0 is locally asymptotically stable, and there exists a positive unstable equilibrium; when $0 < \psi \ll 1$, 0 is unstable and there exists locally asymptotically stable equilibrium;*
2. *$a < 0$, $b < 0$. When $\psi < 0$ with $\|\psi\| \ll 1$, 0 is unstable; when $0 < \psi \ll 1$, 0 is locally asymptotically stable, and there exists a positive unstable equilibrium;*
3. *$a > 0$, $b < 0$. When $\psi < 0$ with $\|\psi\| \ll 1$, 0 is unstable, and there exists a locally asymptotically stable negative equilibrium; when $0 < \psi \ll 1$, 0 is stable, and a positive unstable equilibrium appears;*
4. *$a < 0$, $b > 0$. When ψ changes from negative to positive, 0 changes its stability from stable to unstable. Correspondingly a negative unstable equilibrium becomes positive and locally asymptotically stable.*

The linearisation of system (2) in the neighbourhood of DFE x^1 and around $\mathcal{R}_0 = 1$, using expression in equation (21) setting γ_1 to ζ, yields

$$\frac{dx(t)}{dt} = J(x^1)x(t), \tag{A2}$$

where

$$J(x^1) = \begin{pmatrix} -\frac{r_0\beta}{\mu_M} & 0 & 0 & \frac{\mu_M(\beta+\mu_J)}{\beta} & \frac{\mu_M(\beta+\mu_J)}{\beta} & \mathcal{Q} & \mathcal{Q} & -\frac{\omega_1\nu\mu_M}{\beta+\mu_M} \\ 0 & -k_1 & 0 & 0 & 0 & 0 & 0 & \frac{\omega_1\nu\mu_M}{\beta+\mu_M} \\ 0 & \theta & -k_2 & 0 & 0 & 0 & 0 & 0 \\ \beta & 0 & 0 & -\mu_M & 0 & 0 & 0 & -\frac{\omega_2\nu\beta}{\beta+\mu_M} \\ 0 & \beta & 0 & 0 & -k_3 & 0 & 0 & \frac{\omega_2\nu\beta}{\beta+\mu_M} \\ 0 & 0 & \beta & 0 & \theta & -k_4 & 0 & 0 \\ 0 & 0 & 0 & 0 & 0 & \alpha & -k_5 & 0 \\ 0 & 0 & \zeta & 0 & 0 & \eta\zeta & 0 & -k_6 \end{pmatrix},$$

where $\mathcal{Q} = \frac{\mu_M(\beta+\mu_J)+r_0(\varepsilon-1)\beta}{\beta}$.

The matrix $J(x^1)$ admits $\rho = 0$ as eigenvalue, the other eigenvalues still having a negative real part. Thereby, assumption A_1 of Theorem 6 is verified.

Let us now verify assumption A_2. We need to compute the left and right eigenvectors of matrix $J(x^1)$ associated to the eigenvalue $\rho = 0$. The left eigenvector, denoted by $v = (v_1, v_2, v_3, v_4, v_5, v_6, v_7, v_8)$, satisfies $vJ(x^1) = \mathbf{0}$

Solving the above equation, yields

$$\begin{cases} v_1 = 0, \\ v_2 = \dfrac{\zeta\theta[\beta\eta(k_2+k_3)+k_3k_4]}{k_1k_2k_3k_4}v_8, \\ v_3 = \dfrac{\zeta(\beta\eta+k_4)}{k_2k_4}v_8, \\ v_4 = 0, \\ v_5 = \dfrac{\eta\zeta\theta}{k_3k_4}v_8, \\ v_6 = \dfrac{\eta\zeta}{k_4}v_8, \\ v_7 = 0,\ v_8 > 0. \end{cases}$$

Similarly, the right eigenvector of matrix $J(x^1)$, denoted by $u = (u_1, u_2, u_3, u_4, u_5, u_6, u_7, u_8)^T$, satisfies $J(x^1)u = \mathbf{0}$,

Solving the above equation, we obtain

$$\begin{cases} u_1 = \dfrac{u_8\nu\mu_M\mathcal{X}}{(\beta+\mu_M)((\beta+\mu_M)\mu_M - r_0\beta)k_1k_2k_3k_4k_5}, \\ u_2 = \dfrac{\omega_1\nu\mu_M}{(\beta+\mu_M)k_1}u_8, \\ u_3 = \dfrac{\theta\omega_1\nu\mu_M}{(\beta+\mu_M)k_1k_2}u_8, \\ u_4 = \dfrac{\beta(-\nu\omega_2u_8 + (\beta+\mu_M)u_1)}{(\beta+\mu_M)\mu_M} \\ u_5 = \dfrac{\beta\nu(\mu_M\omega_1+\omega_2k_1)}{(\beta+\mu_M)k_1k_3}u_8, \\ u_6 = \dfrac{\beta\nu\theta(\mu_M\omega_1(k_2+k_3)+\omega_2k_1k_2)}{(\beta+\mu_M)k_1k_2k_3k_4}u_8, \\ u_7 = \dfrac{\nu\theta\alpha\beta(\mu_M\omega_1(k_2+k_3)+\omega_2k_1k_2)}{(\beta+\mu_M)k_1k_2k_3k_4k_5}u_8, \\ u_8 > 0. \end{cases}$$

where

$$\begin{cases} \mathcal{X} = \mathcal{X}_1 + \mathcal{X}_2 + \mathcal{X}_3 + \mathcal{X}_4, \\ \mathcal{X}_1 = (\beta+\mu_J)\omega_1((k_2+k_3)(\alpha+k_5)\theta + k_2k_4k_5)\mu_M^2, \\ \mathcal{X}_2 = ((r_0(\varepsilon-1)\omega_1 + k_1\omega_2)k_2 + \omega_1k_3r_0(\varepsilon-1))\beta + \mu_J\omega_2k_1k_2, \\ \mathcal{X}_3 = ((\alpha+k_5)\theta + k_1k_2k_4k_5(\beta\omega_2 - k_3\omega_1 + \mu_J\omega_2))\mu_M, \\ \mathcal{X}_4 = k_1\omega_2k_2(\beta r_0(\varepsilon-1)(\alpha+k_5)\theta - k_3k_4k_5(\beta+\mu_J)). \end{cases}$$

The expression b defined in Assumption A_2 of Theorem 6 for system (2) is rewritten by

$$b = \sum_{k,i=1}^{8} v_k u_i \frac{\partial^2 F_k}{\partial x_i \partial \gamma_1}(x^1, \zeta),$$

where $F_k = \dot{x}_k$ with $k = 1, 2, ..., 8$ corresponding to system (2).

The only term of partial derivative that is non-null corresponds to

$$v_8\frac{\partial^2 F_8}{\partial x_3\partial\gamma_1}(x^1,\zeta) = v_8 \quad \text{and} \quad v_8\frac{\partial^2 F_8}{\partial x_6\partial\gamma_1}(x^1,\zeta) = v_8\eta.$$

Substituting the above expression into the expression of b, yields

$$b = v_8u_3\frac{\partial^2 F_8}{\partial x_3\partial\gamma_1}(x^1,\zeta) + v_8u_6\frac{\partial^2 F_8}{\partial x_6\partial\gamma_1}(x^1,\zeta) = v_8(u_3 + u_6\eta),$$

Then

$$b = v_8(u_3 + u_6\eta) > 0 \tag{A3}$$

Let us compute the expression of a, defined in Assumption A_2 of Theorem 6 for system (2), which is

$$a = \sum_{i,j,k=1}^{8} v_k u_i u_j \frac{\partial^2 F_k}{\partial x_i \partial x_j}(x^1, \zeta).$$

The only terms that are non-null correspond to

$$\begin{aligned}
v_2 \frac{\partial^2 F_2}{\partial x_1 \partial x_8}(x^1,\zeta) &= v_2 \frac{\partial^2 F_2}{\partial x_8 \partial x_1}(x^1,\zeta) = \frac{\omega_1 \nu M_S^1}{(J_S^1 + M_S^1)^2} v_2 \\
v_2 \frac{\partial^2 F_2}{\partial x_i \partial x_8}(x^1,\zeta) &= v_2 \frac{\partial^2 F_2}{\partial x_8 \partial x_j}(x^1,\zeta) = -\frac{\omega_1 \nu J_S^1}{(J_S^1 + M_S^1)^2} v_2 \quad \text{for } i,j = 2,...,7. \\
v_5 \frac{\partial^2 F_5}{\partial x_4 \partial x_8}(x^1,\zeta) &= v_5 \frac{\partial^2 F_5}{\partial x_8 \partial x_4}(x^1,\zeta) = \frac{\omega_2 \nu J_S^1}{(J_S^1 + M_S^1)^2} v_5 \\
v_2 \frac{\partial^2 F_5}{\partial x_i \partial x_8}(x^1,\zeta) &= v_5 \frac{\partial^2 F_5}{\partial x_8 \partial x_j}(x^1,\zeta) = -\frac{\omega_2 \nu M_S^1}{(J_S^1 + M_S^1)^2} v_5 \quad \text{for } i,j = 2,...,7.
\end{aligned}$$

Substituting these above expressions into the expression of a, yields

$$\begin{aligned}
a &= 2u_8 \left[v_2 \sum_{j=1}^{7} u_j \frac{\partial^2 F_2}{\partial x_j \partial x_8}(x^1,\zeta) + v_5 \sum_{j=1}^{7} u_j \frac{\partial^2 F_5}{\partial x_j \partial x_8}(x^1,\zeta) \right], \\
&= 2u_8 v_2 \left(\frac{\omega_1 \nu M_S^1}{(J_S^1 + M_S^1)^2} u_1 - \frac{\omega_1 \nu J_S^1}{(J_S^1 + M_S^1)^2}(u_2 + u_3 + u_4 + u_5 + u_6 + u_7) \right) \\
&+ 2u_8 v_5 \left(\frac{\omega_2 \nu J_S^1}{(J_S^1 + M_S^1)^2} u_1 - \frac{\omega_2 \nu M_S^1}{(J_S^1 + M_S^1)^2}(u_2 + u_3 + u_4 + u_5 + u_6 + u_7) \right).
\end{aligned}$$

Replace the values of J_S^1, M_S^1, v_2 and v_5, we obtain

$$\begin{aligned}
a = &\frac{2\zeta \mu_M r_1 \omega_1 \nu \beta \theta u_8 v_8 (\mu_M \sum_{i=2}^{7} u_i - \beta u_1)(k_4 k_3 + \eta\beta(k_2 + k_3))}{k_1 k_2 k_3 k_4 (\beta + \mu_M)^2((\beta + \mu_J)\mu_M - \beta r_0))} \\
&+ \frac{2r_1 \theta \mu_M \zeta \beta \nu \omega_2 u_8 v_8 \eta (\beta(u_1 + u_2 + u_3 + u_5 + u_6 + u_7) - \mu_M u_4)}{(\beta + \mu_M)^2((\beta + \mu_J)\mu_M - \beta r_0) k_3 k_4}.
\end{aligned} \tag{A4}$$

The expression b given in equation (A3) is always positive, then the direction of bifurcation depends on the sign of a given by (A4). This means that we are in the case 1 and 4 of Theorem 6.

Appendix B Other types of bifurcation

Beside the forward and backward bifurcation diagrams presented in section 4. Figure B1 shows two different bifurcation diagrams, where the endemic equilibrium disappears for large $\mathcal{R}_0$ values while the trivial equilibrium becomes stable. Subplot (a) presents a forward bifurcation, as in Figure 2; subplot (b) presents a backward bifurcation, as in Figure 4. In both cases, these large $\mathcal{R}_0$ values lead to the plantation destruction. This phenomenon is commonly associated with frequency-dependence Boots and Sasaki (2003); De Castro and Bolker (2005); Ryder et al (2007); Best et al (2012). Boots and Sasaki (2003) explored diseases transmitted via frequency-dependent methods, like sexually transmitted and vector-borne infections, which can evolve to push host populations towards extinction by maximizing their basic reproduction number. Authors proved that, independently from the form of the relationship between transmission and virulence, there is always the possibility of evolution to extinction when transmission is frequency-dependent. De Castro and Bolker (2005) conducted a review identifying the mechanisms of disease-induced extinction. Based on various studies, they concluded that frequency-dependence is a theoretical mechanism driving host extinction. Furthermore, their findings suggested that there is little empirical evidence indicating that diseases transmitted in a frequency-dependent manner pose a significant threat. Ryder et al (2007) demonstrated that in host-parasite systems normally exhibiting density-dependent transmission, parasite-induced extinction could occur when adding a little frequency-dependent transmission. The findings of Best et al (2012) underscore the crucial role of local processes in extinctions driven by parasites. They show that disease extinction may occur both for local density-dependent and frequency-dependent transmission, but that is more likely for the latter.

Nevertheless, we justified our frequency-dependent transmission by a dense plantation. In the process of plantation destruction, this high density assumption is not satisfied anymore, which limits the relevance of this result in the CLR case.

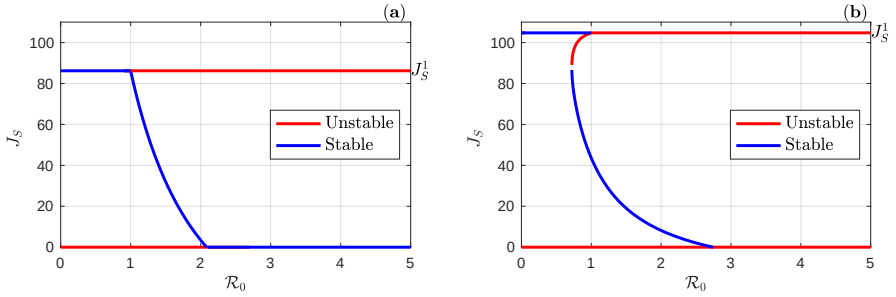

Fig. B1 Subplots present the $(\mathcal{R}_0, J_S)$-bifurcation diagram with stable (blue curve) and unstable (red curve) equilibria of system (1).The bifurcation parameter is γ_1, $\mathcal{R}_0 = \zeta\gamma_1$ and $\gamma_2 = \eta\gamma_1$, with ζ defined in equation (21). Subplot (a) shows a forward bifurcation using parameter values in Table 4 except $\beta = 0.0003$/day and $\alpha = 0.95$ leading to $\zeta = 26.37$ spores/leaf.day. Subplot (b) shows the backward bifurcation using parameter values in Table 4 except $d = 0.8961$ spores/leaf.day leading to $\zeta = 7.77$ spores/leaf.day.

Appendix C Analysis of the model without stage structure

When we remove the stage structure, we obtain a system with five equations, with state variables (S, L, I, U, B):

$$\begin{cases} \dot{S} = r_0 N_1 - r_1 NS - \dfrac{\nu\omega US}{N} - \mu S, \\ \dot{L} = \dfrac{\nu\omega US}{N} - (\mu + \theta)L, \\ \dot{I} = \theta L - (\mu + \alpha)I, \\ \dot{R} = \alpha I - (\mu + d)R, \\ \dot{U} = \gamma I - (\nu + \mu_U)U. \end{cases} \tag{C5}$$

System (C5) is defined in domain

$$\Gamma_n = \mathbb{R}^5_+ \setminus \{(0, 0, 0, 0, U) \text{ with } U \geq 0\}.$$

The DFE of system (C5) is $E_n = (S_n, 0, 0, 0, 0)$, where $S_n = \frac{r_0 - \mu}{r_1}$ exists when $r_0 - \mu > 0$. If the condition does not hold, the coffee plantation cannot survive.

The basic reproduction number of system (C5) is given by

$$\mathcal{R}_{0,n} = \frac{\nu\theta\gamma}{(\mu + \theta)(\mu + \alpha)(\nu + \mu_U)}.$$

Lemma 7 *According to (Van den Driessche and Watmough, 2002), the DFE E_n of system (2) is locally asymptotically stable (LAS) in Γ_n when $\mathcal{R}_{0,n} < 1$, and unstable if $\mathcal{R}_{0,n} > 1$.*

Theorem 8 *If $\mathcal{R}_{0,n} < 1$, the DFE E_n is globally asymptotically stable in region Γ_n and unstable otherwise.*

Proof Consider the cooperative linear subsystem

$$\begin{cases} \dot{L} = \nu\omega U - (\mu + \theta)L, \\ \dot{I} = \theta L - (\mu + \alpha)I, \\ \dot{R} = \alpha I - (\mu + d)R, \\ \dot{U} = \gamma I - (\nu + \mu_U)U, \end{cases} \tag{C6}$$

which is an upper-bound of system (C5) without the first equation, as $\frac{S}{N} \leq 1$. One can easily show that $(0, 0, 0, 0)$ is asymptotically stable if $\mathcal{R}_{0,n} < 1$. Therefore, $(0, 0, 0, 0)$ is GAS in the (L, I, R, U)-subsystem of system (C5).

Substituting $L = 0, I = 0, R = 0$ and $U = 0$ into the first equation of system (C5) yields:

$$\dot{S} = (r_0 - \mu)S\left(1 - \frac{r_1 S}{(r_0 - \mu)}\right).$$

The above logistic equation has two equilibria $S_0 = 0$ and $S_n = \frac{r_0 - \mu}{r_1}$, which are unstable and GAS, respectively. Hence, since the solutions of system (C5) are bounded, $S(t) \longrightarrow S_n$. Thus, one can conclude that the DFE E_n is GAS in region Γ_n for system (C5). □

This analysis shows that there cannot be a backward bifurcation in the system without stage structure (C5).

References

Arino J, McCluskey CC (2010) Effect of a sharp change of the incidence function on the dynamics of a simple disease. Journal of Biological Dynamics 4(5):490–505. https://doi.org/10.1080/17513751003793017

Avelino J, Zelaya H, Merlo A, et al (2006) The intensity of a coffee rust epidemic is dependent on production situations. Ecological modelling 197(3-4):431–447. https://doi.org/10.1016/j.ecolmodel.2006.03.013

Bebber DP, Castillo ÁD, Gurr SJ (2016) Modelling coffee leaf rust risk in Colombia with climate reanalysis data. Philosophical Transactions of the Royal Society B: Biological Sciences 371(1709):2015.0458. https://doi.org/10.1098/rstb.2015.0458

Best A, Webb S, Antonovics J, et al (2012) Local transmission processes and disease-driven host extinctions. Theoretical Ecology 5:211–217. https://doi.org/10.1007/s12080-011-0111-7

Bock KR (1962) Dispersal of uredospores of *Hemileia vastatrix* under field conditions. Transactions of the British Mycological Society 45(1):63–74. https://doi.org/10.1016/S0007-1536(62)80035-7

Boonekamp PM (2012) Are plant diseases too much ignored in the climate change debate? European Journal of Plant Pathology 133(1):291–294. https://doi.org/10.1007/s10658-011-9934-8

Boots M, Sasaki A (2003) Parasite evolution and extinctions. Ecology Letters 6(3):176–182. https://doi.org/10.1046/j.1461-0248.2003.00426.x

Buonomo B, Cerasuolo M (2014) Stability and bifurcation in plant–pathogens interactions. Applied Mathematics and Computation 232:858–871. https://doi.org/10.1016/j.amc.2014.01.127

Burie JB, Calonnec A, Langlais M (2008) Modeling of the invasion of a fungal disease over a vineyard. In: Mathematical Modeling of Biological Systems, Volume II. Modeling and Simulation in Science, Engineering and Technology, Springer, p 11–21, https://doi.org/10.1007/978-0-8176-4556-4_2

Burie JB, Langlais M, Calonnec A (2011) Switching from a mechanistic model to a continuous model to study at different scales the effect of vine growth on the dynamic of a powdery mildew epidemic. Annals of Botany 107(5):885–895. https://doi.org/doi.org/10.1093/aob/mcq233

Calonnec A, Jolivet J, Vivin P, et al (2018) Pathogenicity traits correlate with the susceptible Vitis vinifera leaf physiology transition in the biotroph fungus Erysiphe necator: an adaptation to plant ontogenic resistance. Frontiers in Plant Science 9:1808. https://doi.org/10.3389/fpls.2018.01808

Carisse O, Bouchard J (2010) Age-related susceptibility of strawberry leaves and berries to infection by podosphaera aphanis. Crop Protection 29(9):969–978. https://doi.org/10.1016/j.cropro.2010.03.008

Castillo-Chavez C, Song B (2004) Dynamical models of tuberculosis and their applications. Mathematical Biosciences & Engineering 1(2):361. https://doi.org/10.3934/mbe.2004.1.361

Charrier A, Berthaud J (1985) Botanical classification of coffee. In: Coffee. Springer, chap 2, p 13–47, https://doi.org/10.1007/978-1-4615-6657-1_2

Coleman JS (1986) Leaf development and leaf stress: increased susceptibility associated with sink-source transition. Tree Physiology 2(1-2-3):289–299. https://doi.org/10.1093/treephys/2.1-2-3.289

Cosseboom SD, Hu M (2022) Ontogenic susceptibility of grapevine clusters to ripe rot, caused by the Colletotrichum acutatum and C. gloeosporioides

species complexes. Phytopathology 112(9):1956–1964. https://doi.org/10.1094/PHYTO-01-22-0004-R

De Castro F, Bolker B (2005) Mechanisms of disease-induced extinction. Ecology Letters 8(1):117–126. https://doi.org/10.1111/j.1461-0248.2004.00693.x

Desprez-Loustau ML, Hamelin FM, Marçais B (2019) The ecological and evolutionary trajectory of oak powdery mildew in Europe. In: Wilson K, Fenton A, Tompkins D (eds) Wildlife Disease Ecology: Linking Theory to Data and Application. Ecological Reviews, Cambridge University Press, chap 15, p 429–457, https://doi.org/10.1017/9781316479964.015

Develey-Rivière MP, Galiana E (2007) Resistance to pathogens and host developmental stage: a multifaceted relationship within the plant kingdom. New Phytologist 175(3):405–416. https://doi.org/10.1111/j.1469-8137.2007.02130.x

Djidjou-Demasse R, Lemdjo C, Seydi O (2022) Global dynamics of a spore producing pathogens epidemic system with nonlocal diffusion process. In: Nonlinear Analysis, Geometry and Applications: Proceedings of the Second NLAGA-BIRS Symposium, Cap Skirring, Senegal, January 25–30, 2022, Springer, pp 83–120, https://doi.org/10.1007/978-3-031-04616-2_4

Djuikem C, Grognard F, Tagne Wafo R, et al (2021) Modelling coffee leaf rust dynamics to control its spread. Mathematical Modelling of Natural Phenomena 16:26. https://doi.org/10.1051/mmnp/2021018

Van den Driessche P, Watmough J (2002) Reproduction numbers and subthreshold endemic equilibria for compartmental models of disease transmission. Mathematical Biosciences 180(1-2):29–48. https://doi.org/10.1016/s0025-5564(02)00108-6

Eskes AB (1983) Incomplete resistance to coffee leaf rust. Durable Resistance in Crops pp 291–315. URL https://link.springer.com/chapter/10.1007/978-1-4615-9305-8_26

Farina L, Rinaldi S (2000) Positive linear systems: theory and applications. Pure and Applied Mathematics, John Wiley & Sons, https://doi.org/10.1002/9781118033029

Fleming RA (1980) The potential for control of cereal rust by natural enemies. Theoretical Population Biology 18(3):374–395. https://doi.org/10.1016/0040-5809(80)90060-X

Gubbins S, Gilligan CA, Kleczkowski A (2000) Population dynamics of plant–parasite interactions: Thresholds for invasion. Theoretical Population Biology 57(3):219–233. https://doi.org/https://doi.org/10.1006/tpbi.1999.1441, URL https://www.sciencedirect.com/science/article/pii/S0040580999914417

Gumel A (2012) Causes of backward bifurcations in some epidemiological models. Journal of Mathematical Analysis and Applications 395(1):355–365. https://doi.org/https://doi.org/10.1016/j.jmaa.2012.04.077, URL https://www.sciencedirect.com/science/article/pii/S0022247X12003551

Hacquard S, Petre B, Frey P, et al (2011) The poplar–poplar rust interaction: insights from genomics and transcriptomics. Journal of Pathogens 2011:716,041. https://doi.org/10.4061/2011/716041

Inaba H (2017) Age-structured population dynamics in demography and epidemiology. Springer, https://doi.org/10.1007/978-981-10-0188-8

Kamgang JC (2003) Contribution à la stabilisation des systèmes mécaniques: contribution à l'étude de la stabilité des modèles épidémiologiques. PhD thesis, Université Paul Verlaine-Metz, France, https://hal.univ-lorraine.fr/tel-01749936

Kamgang JC, Sallet G (2008) Computation of threshold conditions for epidemiological models and global stability of the disease-free equilibrium (DFE). Mathematical Biosciences 213(1):1–12. https://doi.org/10.1016/j.mbs.2008.02.005

Koutouleas A, Jörgensen HJL, Jensen B, et al (2019) On the hunt for the alternate host of Hemileia vastatrix. Ecology and Evolution 9(23):13,619–13,631. https://doi.org/https://doi.org/10.1002/ece3.5755

Mammeri Y, Burie J, Langlais M, et al (2014a) How changes in the dynamic of crop susceptibility and cultural practices can be used to better control the spread of a fungal pathogen at the plot scale? Ecological Modelling 290:178–191. https://doi.org/10.1016/j.ecolmodel.2014.02.017, special Issue of the 4th International Symposium on Plant Growth Modeling, Simulation, Visualization and Applications (PMA'12)

Mammeri Y, Burie JB, Langlais M, et al (2014b) How changes in the dynamic of crop susceptibility and cultural practices can be used to better control the spread of a fungal pathogen at the plot scale? Ecological Modelling 290:178–191. https://doi.org/10.1016/j.ecolmodel.2014.02.017

Martcheva M, Inaba H (2020) A Lyapunov–Schmidt method for detecting backward bifurcation in age-structured population models. Journal of Biological Dynamics 14(1):543–565. https://doi.org/10.1080/17513758.

2020.1785024

Maupetit A, Larbat R, Pernaci M, et al (2018) Defense compounds rather than nutrient availability shape aggressiveness trait variation along a leaf maturity gradient in a biotrophic plant pathogen. Frontiers in Plant Science 9:1396. https://doi.org/10.3389/fpls.2018.01396

Nutman FJ, Roberts FM, Clarke RT (1963) Studies on the biology of Hemileia vastatrix Berk. & Br. Transactions of the British Mycological Society 46(1):27–44. https://doi.org/10.1016/S0007-1536(63)80005-4

Pivonia S, Yang X (2006) Relating epidemic progress from a general disease model to seasonal appearance time of rusts in the united states: Implications for soybean rust. Phytopathology 96(4):400–407. https://doi.org/10.1094/PHYTO-96-0400

Ravigné V, Lemesle V, Walter A, et al (2017) Mate limitation in fungal plant parasites can lead to cyclic epidemics in perennial host populations. Bulletin of mathematical biology 79(3):430–447. https://doi.org/10.1007/s11538-016-0240-7

Rayner RW (1961) Germination and penetration studies on coffee rust (Hemileia vastatrix B. & Br.). Annals of Applied Biology 49(3):497–505. https://doi.org/10.1111/j.1744-7348.1961.tb03641.x

Razafindramamba R (1958) Biologie de la rouille du caféier. Revue de Mycologie 23:177–200. URL https://www.documentation.ird.fr/hor/fdi:11779

Rimbaud L, Papaïx J, Barrett LG, et al (2018) Mosaics, mixtures, rotations or pyramiding: What is the optimal strategy to deploy major gene resistance? Evolutionary Applications 11(10):1791–1810. https://doi.org/10.1111/eva.12681

Ryder JJ, Miller MR, White A, et al (2007) Host-parasite population dynamics under combined frequency-and density-dependent transmission. Oikos 116(12):2017–2026. https://doi.org/10.1111/j.2007.0030-1299.15863.x

Sapoukhina N, Tyutyunov Y, Sache I, et al (2010) Spatially mixed crops to control the stratified dispersal of airborne fungal diseases. Ecological Modelling 221(23):2793–2800. https://doi.org/10.1016/j.ecolmodel.2010.08.020

Soh PT, Ndoumbè-Nkeng M, Sache I, et al (2013) Development stage-dependent susceptibility of cocoa fruit to pod rot caused by Phytophthora megakarya. European Journal of Plant Pathology 135:363–370. https://doi.org/10.1007/s10658-012-0092-4

Vandermeer J, Hajian-Forooshani Z, Perfecto I (2018) The dynamics of the coffee rust disease: an epidemiological approach using network theory. European Journal of Plant Pathology 150(4):1001–1010. https://doi.org/10.1007/s10658-017-1339-x

Waller JM (1982) Coffee rust—epidemiology and control. Crop Protection 1(4):385–404. https://doi.org/10.1016/0261-2194(82)90022-9

Wintgens JN (ed) (2009) Coffee: Growing, processing, sustainable production. A guidebook for growers, processors, traders and researchers. Wiley, https://doi.org/10.1002/9783527619627

Zambolim L (2016) Current status and management of coffee leaf rust in Brazil. Tropical Plant Pathology 41(1):1–8. https://doi.org/10.1007/s40858-016-0065-9

Zhang F, Zhao T, Liu H, et al (2019) Backward bifurcation in a stage-structured epidemic model. Applied Mathematics Letters 89:85–90. https://doi.org/https://doi.org/10.1016/j.aml.2018.10.001, URL https://www.sciencedirect.com/science/article/pii/S0893965918303410